Journal of Astrophysics and Astronomy

Self-triggering approach of cosmic ray radio emission at Semnan University Radio Array Experiment

--Manuscript Draft--

Manuscript Number:	JOAA-D-24-00193
Full Title:	Self-triggering approach of cosmic ray radio emission at Semnan University Radio Array Experiment
Article Type:	Original Study
Abstract:	Radio detection of cosmic rays investigates the electromagnetic component of extensive air showers. It is possible to obtain the most critical properties of a cosmic ray, including the depth of shower maximum, energy, and type of primary particle, from radio measurements. Semnan University Radio Array is a new experiment that strives to detect radio emissions from extensive air showers induced by ultra-high energy cosmic rays. As artificial radio frequency interferences usually contaminate radio pulses emitted from charged particles in an extensive air shower, a particular set of devices and sophisticated digital signal processing steps must be in place to exploit the full potential of the radio detection approach in a self-trigger setup. This paper describes the implemented self-triggering approach in SURA-4 to preserve cosmic ray candidates while removing unwanted emissions by utilizing the capabilities of analog and digital elements and incorporating a custom program for radio signal analyses.

J. Astrophys. Astr. (0000) **000**:
DOI

Self-triggering approach of cosmic ray radio emission at Semnan University Radio Array experiment

M.Mostafavi Alhosseini[1], G.Rastegarzadeh[1,*]

[1]Faculty of Physics, Semnan University, Semnan, Iran.

[*]Corresponding author. E-mail: grastegar@semnan.ac.ir

Abstract. Radio detection of cosmic rays investigates the electromagnetic component of extensive air showers. It is possible to obtain the most critical properties of a cosmic ray, including the depth of shower maximum, energy, and type of primary particle, from radio measurements. Semnan University Radio Array is a new experiment that strives to detect radio emissions from extensive air showers induced by ultra-high energy cosmic rays. As artificial radio frequency interferences usually contaminate radio pulses emitted from charged particles in an extensive air shower, a particular set of devices and sophisticated digital signal processing steps must be in place to exploit the full potential of the radio detection approach in a self-trigger setup. This paper describes the implemented self-triggering approach in SURA-4 to preserve cosmic ray candidates while removing unwanted emissions by utilizing the capabilities of analog and digital elements and incorporating a custom program for radio signal analyses.

Keywords. Cosmic ray—Radio antenna array—Air showers—Sself-trigger—Semnan University Radio Array (SURA)—DSP.

1. Introduction

Radio detection of cosmic rays has a long history. The emission of electromagnetic radiation from air showers in the MHz frequency range was first observed in 1965 (Jelley *et al.* 1965). Followed by that, radio detection has been considered a new approach that could compensate for the disadvantages of other techniques with its high-duty cycle, cost-effective setup, and the possibility of obtaining essential cosmic ray properties from radio measurements. However, theoretical and experimental difficulties and the emergence of the fluorescence light detection of cosmic rays that provided robust performance led to a nearly complete cessation of interest in this approach (Huege 2018). This situation changed with the development of the new set of radio experiments over the past two decades (Abreu *et al.* 2012). Computer modeling also played an essential role in understanding the physics of radio emissions from cosmic rays in parallel to experimental activities (Huege 2005).

It is believed that the time-varying transverse current initiated by the acceleration and deceleration of electrons and positrons under the presence of the Earth's magnetic field is the primary mechanism of radio emission from an Extensive Air Shower (Huege 2013). These radio emissions propagating in a forward direction are coherent in frequencies up to 100 MHz (Huege *et al.* 2017). The radio pulses emitted in such circumstances have a duration of about ten to 100 ns. The power of the received signal from an air shower directly relates to the square of the primary particle energy.

Different experiments tried to benefit from the advantages of radio detection of cosmic rays. From the first generation of radio experiments, including LOPES (Falcke *et al.* 2005), and CODALEMA (Ardouin *et al.* 2005), to the new set of radio experiments, such as AERA (Fliescher 2012) and LOFAR (Van Haarlem *et al.* 2013), searching for the possible development of a whole autonomous radio setup has always been a field of interest in various experiments. Some experiments have made intensive efforts to exploit the full potential of radio detection techniques by implementing self-rigger algorithms to detect cosmic rays. Although few experiments have reported the successful detection of cosmic rays in a self-trigger setup (Ardouin *et al.* 2011), searching for new approaches to developing a fully autonomous radio setup is still underway.

The Semnan University Radio Array (SURA) is a new cosmic ray experiment in the Middle East (Rastegarzadeh *et al.* 2020). The ultimate objective of this project is to study and detect radio emissions from extensive air showers induced by ultra-high energy cosmic rays above 10^{17} eV. A few different stages have been considered for the SURA project, which expands the overall detection area while adding new capabilities to the experiment over the coming years. The project's

first phase, SURA-4, currently works in a self-triggered mode. In this study, we describe the capabilities of the SURA-4 electronics, particularly with the self-trigger perspective, and discuss the digital signal processing stages in the current setup.

Section 2 briefly discusses the SURA-4. In section 3, we introduce bandwidth considerations for the experiment. In section 4, we investigate the properties of the analog devices, including a detailed simulation result of the LPDA antennas. In the following two sections, we discuss the digital signal processing stages. First, section 5 describes the online signal analysis using the capabilities of a Field Programmable Gate Array (FPGA), while section 6 covers offline signal analysis using a custom-developed code. Finally, we conclude our discussion in the last section.

2. SURA-4 prototype

The main objective of the SURA-4 prototype is to verify the feasibility of air shower detection in a small-scale radio array and investigate the challenges in an experimental setup while developing the necessary algorithms to distinguish extensive air shower emissions from background noise. Despite severe challenges, SURA aims to develop a self-triggering radio array that would exploit the full potential of the radio detection approach.

A specific set of devices and algorithms must be in place to achieve an utterly autonomous array. SURA-4 benefits from custom-made east-west oriented log-periodic dipole antennas deployed on the roof of the physics faculty. In addition, a read-out system, and custom programs, have been deployed and developed to receive and analyze radio pulses.

Fig. 1 shows a schematic view of the SURA-4 system design, including the electronic and digital signal processing stages to distinguish extensive air shower emissions from unwanted emissions. We discuss each part in detail in the following sections.

3. Bandwidth consideration

A key element in establishing a self-trigger setup is carefully selecting the operation bandwidth considering the background Radio Frequency Interferences (RFIs) at the location of the experiment. Determining the proper frequency window is vital to eliminate unwanted radio emissions while reaching the maximum signal-to-noise ratio. This factor also plays a crucial role in the type and design of the experiment's antennas. It is evident that the location of the experiment and the

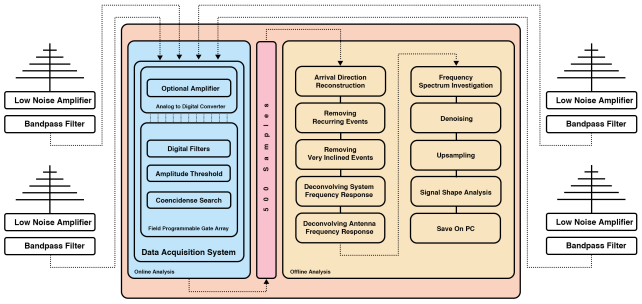

Figure 1: A simple schematic of the SURA-4 system. Digital signal processing consists of two phases. The first is implemented using the capabilities of an FPGA in an online mode. The second is an offline investigation of the recorded samples using a custom-developed code.

corresponding RFIs also plays an essential role in the operating bandwidth selection.

Since it was necessary to access and maintain the array in the first stage and keep the cost of the experiment under control, we had to deploy SURA-4 inside the Semnan University campus. However, it is planned to move the array to a more radio-quiet location in the future upon the successful operation of the experiment's first phase. Previous studies showed that extensive air showers emit coherent radio emissions in the frequency range below 100 MHz (Huege *et al.* 2007). Other experiments' measurements also indicated that it is expected to observe intense background noise at a few hundred up to 30 MHz (Abreu *et al.* 2012).

Upon designing and deploying the LPDA antennas, it was possible to precisely measure the frequency spectrum at the location of the SURA-4 experiment. Fig. 2 shows the power spectral density measured on the roof of the physics faculty with one of the SURA-4 log-periodic dipole antennas. The up plot is captured by the SURA-4 data acquisition system, while the bottom plot is measured with a digital oscilloscope at 230 MSPS.

Three critical points can be concluded from this figure; the first is the substantial pollution of the frequency spectrum in the frequency range of a few hundred up to nearly 30 MHz. The second is the presence of almost fixed mono-frequent emissions in the frequency range of 56 to 76 MHz. We can confirm that the power and position of these emissions remained nearly unchanged over time. We concluded that analog TV transmitters initiated these emissions. Furthermore, strong FM emissions are also visible in frequencies above 80 MHz in the bottom pane of this figure. To have the maximum possible signal-to-noise ratio and by considering the electronics' technical specifications in the SURA-4 setup, we decided to choose the 40-80 MHz frequency window as the operation bandwidth of the SURA-4 ex-

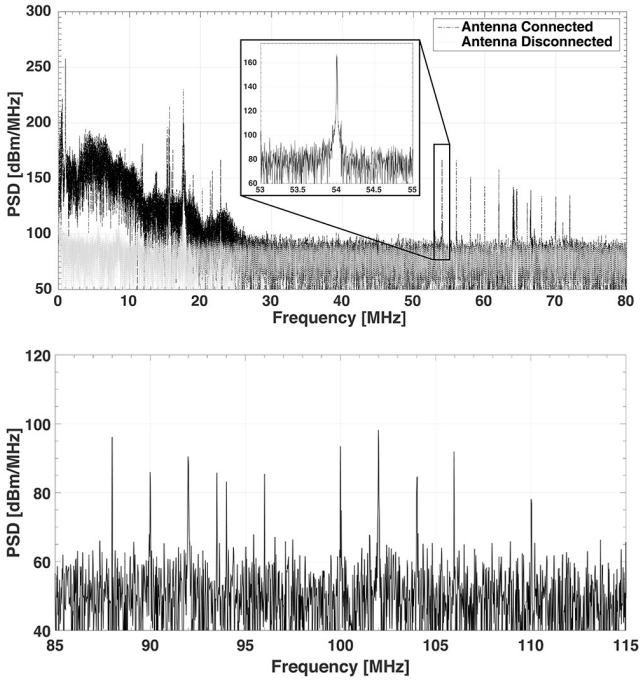

Figure 2: Measured Power Spectral Density at the location of the SURA-4 with one of the LPDA antennas. The spectrum shown in the up pane is measured by SURA-4 DAS. The bottom spectrum is captured using a digital oscilloscope running at 230 MSPS to showcase the presence of the FM emission.

periment.

4. Analog devices

The first element of the SURA-4 setup is an antenna that receives radio emissions from extensive air showers. The custom-made SURA-4 LPDA antennas are sensitive to radio emissions in a 40-80 MHz frequency window. The operative bandwidth of an antenna can be described by measuring the real (R_s) and imaginary (X_s) parts of the antenna's impedance at desired frequencies. Such measurement can be used to obtain the reflected power of an antenna:

$$ReflectedPower = (\frac{Z_L - Z_0}{Z_L + Z_0})^2 * 100 \quad (1)$$

Where: Z_L=R_s + jX_s and characteristic impedance of coaxial cables, LNA and BPF (Z_0), equal 50Ω. We used an antenna analyzer to measure this parameter in 2000 frequency points from 20 to 100 MHz and compared the results with computer simulations in the same frequency bins. The details about SURA-4 LPDA modeling in ALTAIR FEKO software can be found in (Sabouhi *et al.* 2022).

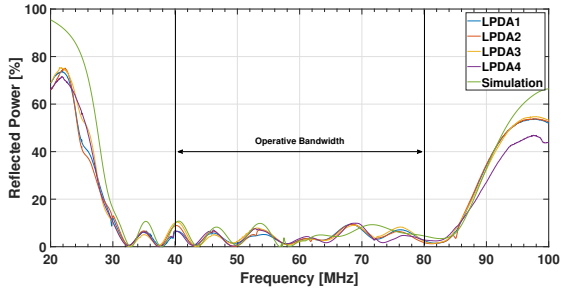

Figure 3: Measured and simulated reflected power of the SURA-4 LPDA antennas.

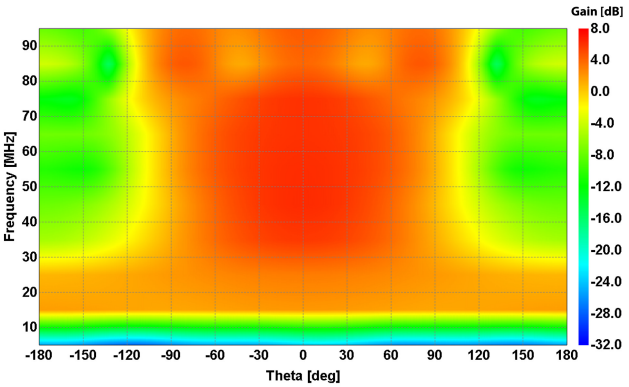

Figure 4: Simulated total gain of the LPDA antenna in 1-100 MHz for ϕ=90°.

more on LPDA construction (huge?)

Fig. 3 shows a comparison between the simulated model's reflected power and the deployed unit's measurement. It is also visible that the antennas have the best reception for the emissions in the 40-80 frequency band. Furthermore, as a result of good build quality, we observe similar behavior from all four units.

Besides having an appropriate operative bandwidth and high gain, the SURA-4 LPDA antennas are more sensitive to radio emissions from smaller zenith angles. Fig. 4 demonstrates the simulated LPDA antenna's surface plot from 1 to 100 MHz, which shows the unit's total gain in different frequencies for azimuth angle (ϕ) 90°. It is shown that the antenna gain decreases gradually as we move toward the horizon (θ=-90,90). In contrast, the antenna has higher gain values as we move to zenith angles close to zero. As many artificial emissions originate from sources close to the horizon, this feature helps reduce major false-triggering from unwanted emissions. cant angle?

The SURA-4 setup also benefits from low-noise amplifiers and bandpass filters directly attached to the LPDA antennas. These units preserve weak radio signals while removing a significant part of unwanted emissions. Furthermore, using analog filters helps to reduce the amount of data that needs to be digitally pro-

plot of noise figure? absolute noise spectral density vs, -174 dBm/Hz?

cessed. The low noise amplifier has a steady gain of 29.02 dB. The bandpass filter passes emissions in the 44-79 MHz and highly rejects radio emissions outside this band. The frequency response of each unit in the SURA-4 electronic chain has been measured, and the overall system frequency response has been obtained, which makes it possible to reconstruct the electric field strength and compare the measurements with simulation results (Sabouhi *et al.* 2022).

5. Digital signal processing

The digital signal processing is split into two parts to ensure that the digital Data Acquisition System (DAS) is not overburdened. The first is a real-time online data analysis, and the second is an offline survey of recorded samples passed through the criteria of the first stage. In this section, we discuss the procedures in each phase.

5.1 *Online digital signal processing*

The online digital signal processing is performed using an Intel Arria V GZ Field-Programmable Gate Array (FPGA). The 32 GB of random access memory on the board makes capturing up to 14 seconds of continuous data possible. This feature ensures the minimum dead time during signal analyses.

The FPGA is directly connected to an Analog-to-Digital Converter (ADC). The ADC unit has high linearity, consumes very low power, has four-channel, each with a 14-bit vertical resolution, and captures data with up to 160 MSPS.

These units are designed to handle demanding high-frequency input signals with high dynamic range requirements. This category of ADCs supports serial Current-Mode Logic (CML) and JESD204B interfaces to reduce the number of interface lines. The ADC34J45 used in the SURA-4 setup support interface speeds up to 3.2 Gbps.

The online analysis stage includes three main steps:

- Digital filters
- Amplitude threshold decision
- Coencidense search

5.1.1 *Digital filters* Although SURA-4 uses analog bandpass filters, we have also designed two types of digital filters to tackle strong emissions below 30 MHz and suppress mono-frequent emissions beyond 54 MHz.

The first is an adjustable high-pass filter that can be turned on/off during data capture. In SURA-4, this filter is currently set to 40 MHz to reject emissions in the few hundred MHz frequency bands.

The second is a notch filter designed to suppress fixed mono-frequent emissions. It is possible to add, remove or modify the number or frequency properties of the notch filters if the position or behavior of an unwanted emissions changes or a new spike appears in the frequency spectrum. Using a chain of notch filters makes it possible to reject specific frequencies without adding artificial values to the spectrum.

what is notch? RLC are very temp dependent

5.1.2 *Amplitude threshold decision* The second part of the online analysis process is performed by implementing an adjustable threshold decision parameter. The SURA-4 currently searches for radio emissions with a specific signal-to-noise ratio. Considering the noise level, the user defines a threshold per run. The program constantly searches for signal amplitude above the predefined threshold and marks the position of the peaks in the recorded samples. If a peak amplitude is higher than the defined threshold and the sample number of the peaks from all antennas falls inside a predefined time frame (Section 5.1.3), an adjustable number of samples will be recorded. This number is currently set to 500 samples equal to 3.125 μs. 160 MSa

5.1.3 *Coencidense search* A coencidense search is also performed based on the received radio signal's primary peak location during online digital signal processing. Since we use equal cable length in the SURA-4 layout, no delay is expected in the received signals from four LPDA antennas. As a result, the radio signal from a singular extensive air shower is expected to be received by the antennas within a particular time frame based on the zenith and azimuth angle of the shower.

Radio signals emitted from a vertical air shower should be received almost simultaneously. In contrast, for an inclined air shower propagating parallel to the horizon, the signal should be detected in a time window equal to $|t_i - t_j| \leq \frac{d_{ij}}{c}$, Where d_{ij} is the distance between the two antennas that are farthest apart, t_i and t_j are the time when the amplitudes reach its maximum value in respective antennas, and c is the speed of light.

By narrowing the coencidense search time window, it is possible to avoid strong man-made emissions coming at a large zenith angle close to the horizon. However, this could result in losing some potential cosmic ray candidates. The decision to remove emissions with sources close to the horizon is made during offline Digital Signal Processing (DSP) (section 6.4)

As a result of the online DSP procedures, a series of files will be saved for further offline analysis. One example of the recorded samples is shown in Fig. 5. Four crucial points can be concluded from this figure:

this look likes more than kTB for 29 dB gain

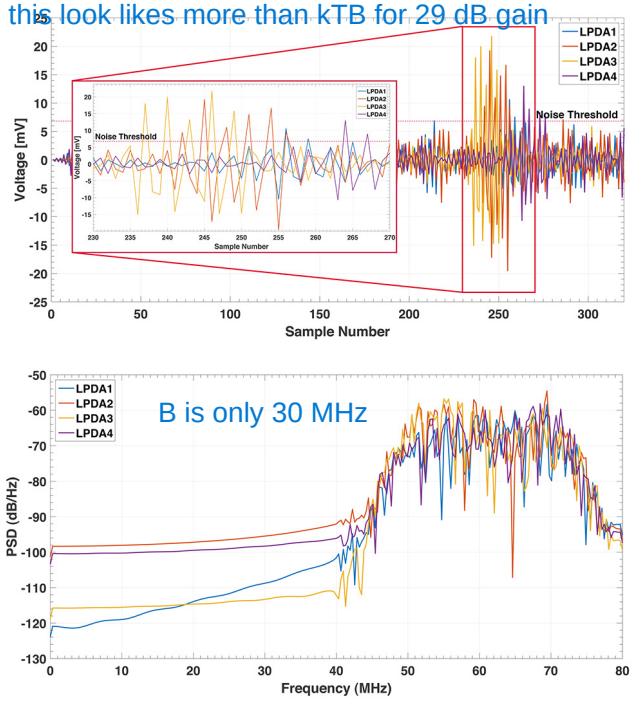

Figure 5: The up plot shows the time-domain figure of a random sample during the online digital signal processing stage. The noise threshold level of the SURA experiment is shown with a dashed red line. The bottom figure is the power spectral density of the same sample. The effects of the digital and analog filters are visible. In particular, notch filters have effectively removed all mono-frequent emissions, as no particular spike is present in this figure.

pre-post notch filter waveform?

1. During this capture, the digital high pass filter has been utilized to eliminate strong emissions at low frequencies. The bottom plot shows the power spectral density of this particular sample where the effect of the digital high pass filter is visible.

2. As a result of using a series of notch filters, the frequency spectrum of the racorded data has been cleared from significant spikes at the upper part of operative frequency windows, previously visible in the up pane of the Fig. 2.

3. The peak amplitude from all four stations is above the defined threshold shown with a dashed red line in the up figure.

4. The main peak from all four antennas is inside the defined time window, set to 187.5 ns in this capture.

6. Offline digital signal processing

The second part of DSP is performed by the SurA offLine Analyse prograM (SALAM). The current version of this program analyses the recorded samples in nine stages, as described in the following subsections.

6.1 *Arrivial Direction Reconstruction*

Among various mechanisms responsible for the propagation of radio pulses from secondary charged particles in an extensive air shower, the earth's magnetic field plays a vital role, particularly on radio ground footprint (Sabouhi *et al.* 2017). The angle between an extensive air shower axis and the earth's magnetic field vector, known as the geomagnetic angle, affects the emitted radio pulse strength from charged particles as an extensive air shower propagates through the atmosphere. Particles moving parallel to the earth's magnetic field vector receive much smaller Lorentz force than particles moving perpendicularly. The properties of the earth's magnetic field vector at the SURA site are θ_b=36°, ϕ_b=176°. These values are similar to a cosmic ray site in Europe, such as LOPES, where the magnetic field vector equals θ_b=25°, ϕ_b=180°. As a result, we expect the recorded samples to have similar angular distributions in both sites.

Considering the SURA-4 layout and the maximum distance between the antenna, we have implemented a plane radio wavefront in our analysis. We have previously shown that in such circumstances, it is possible to reconstruct the zenith and azimuth angle of the SURA events with an accuracy of about one degree (Rastegarzadeh *et al.* 2020). As the antenna's gain is a function of both the frequency and arrival direction, reconstructing this parameter is vital during offline digital signal processing.

Fig. 6 shows an initial estimation of the arrival direction from 59422 recorded samples recorded from online DSP procedures. The angular distribution of these samples shows a good agreement with published results from the LOPES experiment (Apel *et al.* 2010). This result strengthens the possibility that recorded events originate from charged particles undergoing the earth's magnetic field.

Is absolute flux about right?

6.2 *Recurring events*

The SALAM program's second stage finds and removes recurring events. The program can carry out this task in one of the two following ways, depending on the user's preferences:

1-Time window: In this mode, the time stamp of each recorded sample will be checked versus the rest of the data to find busy periods. Based on the specified

Error bars?

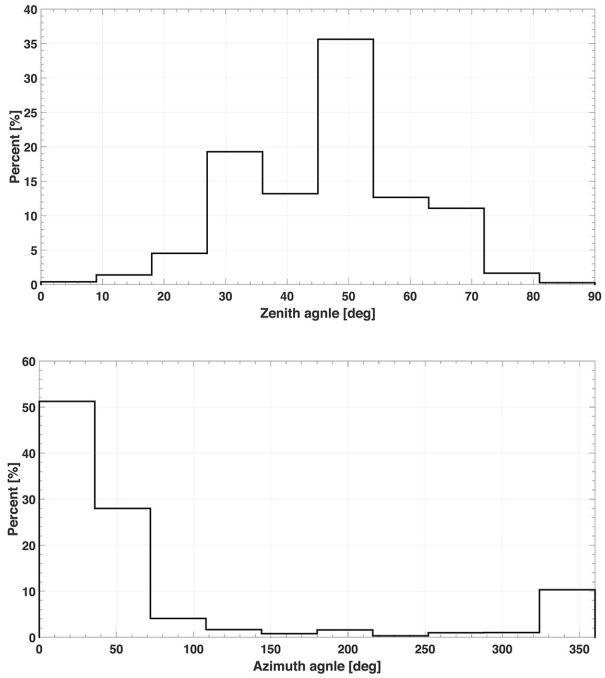

Figure 6: Angular distribution of zenith and azimuth angles of 59422 recorded samples during SURA-4 online DSP stage.

Compare with simulations?

time window, the program excludes samples if more data is stored than the allotted limit in a confined period. Currently, SURA has chosen this method as its default approach. If more than three recorded samles are recorded during three minutes, it will be marked as a busy period, and the corresponding samples will be eliminated.

2-Time-angular window: In this mode, If recorded samples are recorded within a defined time interval, and the reconstructed arrival direction falls within a specific range, the recorded samples will be marked as recurring and get removed from the dataset.

6.3 *Very inclined events*

Inclined air showers can illuminate a much larger area, making them more suitable for radio detection in a large-scale experiment (Sabouhi *et al.* 2015). However, considering the distribution of cosmic rays as a function of the zenith angle, the overall detection area of the SURA-4 experiment, and since significant artificial emissions usually originate from sources close to the horizon, we exclude events with very high reconstructed zenith angle. This adjustable parameter is currently set to 75 degrees.

6.4 *Deconvolving system frequency response*

As described in Section 2, the SURA-4 consists of different elements which can alter the recorded signal's properties. Based on the measurements described in (Sabouhi *et al.* 2022), the user can select and correct the effects of present elements during data capture. This process is done by applying a Fast Fourier Transform (FFT) on the signal before correcting the signal property in the frequency domain.

6.5 *Deconvolving antenna frequency response*

The relation between the received voltage trace at an antenna terminal and the incident electric field can be described by Antenna Factor (AF) parameter:

$$A_F = \frac{E_{incident}}{V_{Recevied}} \tag{2}$$

The antenna's gain and frequency can describe the antenna factor equation. The power density of the incident wave can be described as:

$$S_{incident} = \frac{|E^2|}{\eta}, \eta = \sqrt{\frac{\mu_0}{\epsilon_0}} \approx 377\Omega \tag{3}$$

Where η is the intrinsic impedance of the free space, which can be described in terms of permittivity and permeability. The captured power by the antenna from the incident wave depends on the effective aperture of the antenna:

$$P_{recevied} = S_{incident} A_e \tag{4}$$

and

$$A_e = \frac{\lambda^2}{4\pi} G \tag{5}$$

So considering that:

$$P_{Recevied} = S_{Incident} \frac{\lambda^2}{4\pi} G = \frac{V^2}{Z_{Load}} \tag{6}$$

One can calculate that:

$$A_F = \sqrt{\frac{4\pi\eta f^2}{c^2 G Z_{Load}}} \tag{7}$$

ALTAIR FEKO

Calculating the antenna gain for each desired frequency is necessary to deconvolve the antenna response. As a result, a detailed modeling and simulation of the LPDA antenna using ATLAR FEKO software has been done, and the antenna gain has been calculated for frequencies from 1 to 80 MHz and all possible incoming directions. The antenna factor will be calculated after taking

cf -114 dBm/Hz? y-units?

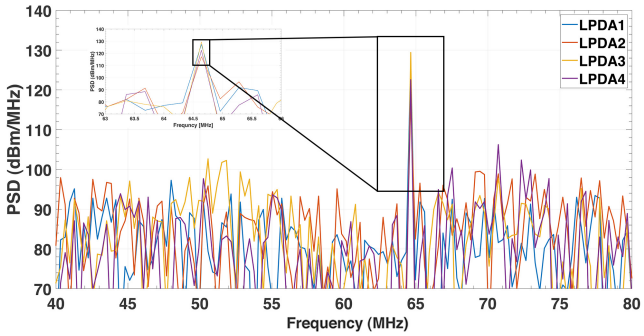

Figure 7: An example recorded sample during the frequency spectrum investigation step. A spike is visible at 64.64 MHz.

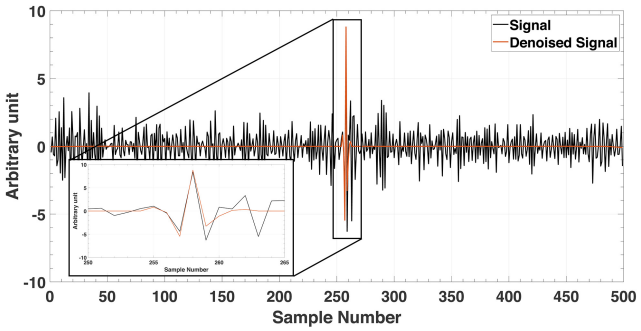

Figure 8: The black line represents a sample passed through different stages of online and offline DSP. The brown line shows the denoised signal. The small figure in the bottom left corner zooms around the vicinity of the central signal peak.

an FFT and obtaining the intended frequencies for each recorded sample based on the number of samples. Each recorded sample contains 500 samples in the current format, resulting in 251 unique frequencies in the frequency domain. After applying the antenna response, an inverse Fourier transform will take the signal back to the time domain and continue the digital signal processing steps.

6.6 *Frequency spectrum investigation*

Next, we investigate the frequency spectrum to look for the possible emergence of transient carriers or to observe the effects of other sources skipped during the online DSP stage. As a result of notch filters and the expected coherence radio emissions from extensive air showers below 100 MHz, we anticipate recording a relatively flat frequency spectrum. We exclude the recorded samples not showing such spectrum behavior by setting an adjustable threshold on the magnitude of received radio pulses in the frequency domain. The events with a higher magnitude than the predefined values will be marked for further analysis. Fig. 7 shows an example where the threshold is set to 20 dB. A spike is visible at 64.64 MHz. SALAM marks the position of new spikes and saves them alongside the file name for further analysis.

6.7 *Denoising*

Noise treatment is a significant challenge in a self-trigger setup. Different experiments have investigated various approaches to tackle this issue, from the interferometry technique in early experiments (Schröder *et al.* 2015) to machine learning in recent years (Erdmann *et al.* 2019). SALAM implements an approach based on the wavelet technique to process the denoising on a per-event/channel basis.This approach has also been used in particle detection (Rastegarzadeh *et al.* 1998) and more recently in radio detection (Watanabe *et al.* 2021) of cosmic rays. Compared to the machine learning-based approaches, this technique does not require a large set of data needed to train the sophisticated algorithms in machine learning-based methods, making it more suitable for a small-scale experiments like SURA. Furthermore, this model-free approach is more adjustable in case a change happens in the property of the noise, mainly because the SURA experiment is in the prototype stage. Different types of wavelets with various threshold methods were investigated to find a combination of wavelet parameters that work best on SURA-4 data. One example is shown in Fig. 8, where the background has been removed while the desired radio signal is almost fully reconstructed.

6.8 *Upsampling*

Reconstructing the best possible signal shape is a crucial step that may lead to determining the depth of shower maximum and, finally, the type of primary particle. Different digital-based methods such as linear interpolation, zero-hold method, and interpolation filter can be used to overcome the hardware limitation in capturing analog signals with a very high sample rate. Although the characteristics of SURA-4 DAS ensure proper digitization, we upsample the data to reconstruct the signal's best possible shape based on an interpolation filter technique. This approach ensures that the upsampled data can be analyzed in both time and frequency-domain.

6.9 *Signal shape analysis*

The last part of the SALAM code performs a signal shape analysis by applying a Hilbert envelope of the upsampled data on a per-event per-channel basis. The method is similar to the template-fitting approach

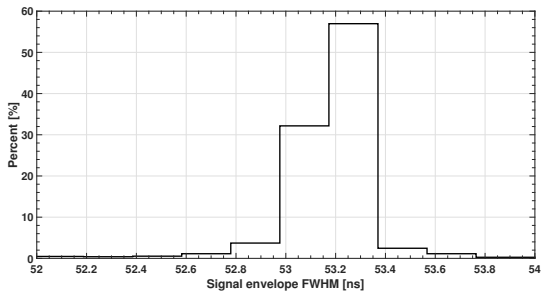

Figure 9: Histogram of signal FWHM from computer simulation at the location of SURA site in 40-80 MHz.

used by the Tunka-Rex experiment (Bezyazeekov *et al.* 2017).

We simulated 378 air showers using CORSIKA 7.74 (Heck *et al.* 1998) and CoREAS 1.4 (Huege *et al.* 2013) with GHESHIA 2002d and QGSJET II-04 (Ostapchenko 2006) as low and high-energy interaction models with thinning set to 10^{-6} and time resolutions of 0.2 ns. The properties of the SURA-4 site, including the earth's magnetic field parameters and antenna locations, have been observed in the simulations.

Proton and Iron were used as primary particles. All simulated events are from air showers with three primary energies of 2.10^{17}, 5.10^{17} and 10^{18}eV, as SURA is intended to operate at energies above 10^{17} eV. We investigated θ equal to 0,30 and 60 and a wide range of ϕ from 0 to 315 degrees with 12 random core location in our simulations. As shown in Fig. 9, we obtained the majority of the filtered signal pulse to have a Hilbert envelope width of 52.4 to 53.8 ns at the location of the SURA experiment.

Besides investigating the width of the Hilbert envelope, SALAM can also investigate the rise and fall time of the denoised signal and check whether the signal properties match the simulation expectations.

7. Running SALAM program on SURA preminilary data

The final goal of the SLAM program is to deconvolve the frequency response of the SURA devices while removing undesired events possibly originating from sources other than a cosmic ray while dealing with the undesired noise and reconstructing the best possible shape of the signal. We investigated the performance of the SALAM program on a sample data set from the SURA experiment. A total number of 59422 recorded samples were investigated, and the following results were obtained:

- Reconstructing the zenith and azimuth angle of the data set showed good agreement with the expected distribution of events possibly originating from charged particles undergoing the earth's magnetic field.
- During the program's second stage, 54032 recorded samples were removed due to setting the initial criteria as if more than three events were recorded in a 3-minute time frame.
- By setting the desired zenith angle up to 75 degrees, the program removed 86 recorded samples with a reconstructed zenith angle of more than 75 degrees.
- Investigating the frequency spectrum of the remaining data set showed that the 1822 recorded samples had undesired spikes with a magnitude higher than the defined threshold.
- During the fifth and sixth stages of the SALAM program, the number of recorded samples did not change. However, the signal property was adjusted due to deconvolving the frequency response of the devices and LPDA antennas.
- During the denoising stage, the level 5 sym wavelet was applied with the Universal threshold denoting method combined with the hard thresholding rule and level-independent noise estimate approach.
- The data were upsampled from the original 6.25 ns to 0.2 ns using the interpolation filter technique.

this must be a strong function of geometry?

- Based on simulation results, we defined a window from 52.4 to 53.8 for FWHM of the signal Hilbert envelope.

The described procedure removed 99.93 percent of total samples under chosen circumstances. Fig.10 shows one example of a sample saved after processing all the stages described in this study. For this particular sample, the denoised upsampled signal has a signal envelope equal to 52.97 ns, which falls within the criteria defined in the SALAM program.

8. Conclusion

SURA-4, the first phase of the Semnan University Radio Array, seeks the feasibility of implementing a self-trigger setup to receive radio signals emitted from charged particles in an extensive air shower.

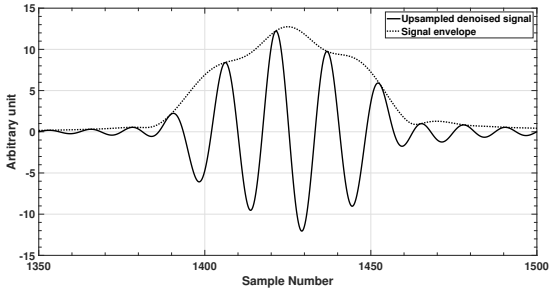

Figure 10: A sample recorded by SURA-4. The denoised upsampled, and signal envelope is shown in black and blue, respectively.

In this study, we investigated the characteristics of SURA-4 analog devices before discussing the digital signal processing steps managed to remove man-made radio frequency interferences. First, we demonstrated the broadband sensitivity of the LPDA antennas in the 40-80 MHz with high attenuation outside this frequency window. We also demonstrated the high gain of the LPDA antennas towards emissions from a smaller zenith angle which would prevent emissions originating close to the horizon from triggering the setup.

The main phase of the SURA-4 self-triggering process is based on sophisticated digital signal processing. In SURA-4, we performed these procedures in two phases. During the first stage, two types of digital filters were designed. The first is a high-pass filter developed to eliminate primary man-made emissions in frequencies up to 30 MHz. The second is a notch filter used in a chain to suppress emissions from mono-frequent carriers in high frequencies. Furthermore, two criteria were discussed, including threshold decision and coencidense search.

We also discussed the steps in the second digital signal processing phase, performed in 9 stages. After reconstructing the arrival direction, we searched for recurring and very inclined events possibly originating from man-made sources. Next, we applied the SURA-4 system response and antenna frequency response to the recorded samples before investigating the frequency spectrum of the samples to find the emergence of possible transient carriers. SURA-4 denoises the recorded signal based on the wavelet technique. We discussed the implementation of this technique on SURA-4 data before upsampling the recorded signal using interpolating filter technique. The last part of our custom-developed code is dedicated to signal shape analysis based on comparing the measurement with the computer simulations. The simulation result showed that the width of the Hilbert envelope on a radio pulse originating from an extensive air shower at the SURA experiment's location should range from 52.4 to 53.8 ns. We used these values as input parameters in the SALAM program to find possible cosmic ray candidates.

Acknowledgments

The authors would like to thank Mohammad Sabouhi for his contributions to data analysis and proofreading of the manuscript.

References

Jelley J.V., *et al.* 1965 Nature Publishing Group UK London, 205, 327.

Huege T., 2018, Proceedings of 2016 international conference on ultra-high energy cosmic rays (uhecr2016), 011031.

Abreu P., *et al.* 2012, Journal of Instrumentation, 7, 10011.

Huege T., 2005, Astroparticle Physics, 24, 116.

Huege T., 2013, AIP Conference Proceedings, 1535, 121.

Huege T., *et al.* 2017, Progress of Theoretical and Experimental Physics, 2017, 12A106.

Falcke H., *et al.*, 2005, Nature, 435.7040, 313.

Ardouin D., *et al.*, 2005, Nuclear Instruments and Methods in Physics Research Section A: Accelerators, Spectrometers, Detectors and Associated Equipment., 55.1-2, 148.

Fliescher S., 2012, Nuclear Instruments and Methods in Physics Research Section A: Accelerators, Spectrometers, Detectors and Associated Equipment, 662, S124.

Van Haarlem M., *et al.* 2013, Astronomy & astrophysics. 556, A2.

Ardouin D., *et al.* 2011, Astroparticle Physics, 34.9, 717.

Rastegarzadeh G., *et al.* 2020, Experimental Astronomy,49.1, 21.

Huege T., *et al.* 2007, 7.11, P11023.

Abreu P., *et al.* 2012, Journal of Instrumentation, 7 (11), P11023.

Sabouhi M., *et al.* 2022, Journal of Astrophysics and Astronomy, 43.2, 56.

Sabouhi M., *et al.* 2017, 35th Int. Cosmic Ray Conf.(ICRC)., 301, 568.

Apel W. D., *et al.* 2010, Astroparticle Physics, 32.6, 294.

Sabouhi M., *et al.* 2015, The 34th International Cosmic Ray Conference, 236.

Schroder F., *et al.* 2015, 34th International Cosmic Ray Conference (ICRC2015), 34, 317.

Erdmann M., *et al.* 2019, Journal of Instrumentation, 14.04, P04005.

Rastegarzadeh G., *et al.* 2001, Journal of Physics G: Nuclear and Particle Physics 27, 2065.

Watanabe C. K. O., *et al.* 2021, 37th International Cosmic Ray Conference (ICRC 2021), Online, 12.07-23.07.

Bezyazeekov P. A., *et al.* 2017, arXiv preprint arXiv:1701.05158.

Heck D., *et al.* 1998, Report fzka. 6019.11.

Huege T., *et al.* 2013, AIP Conference Proceedings, 1535.1, 128.

Ostapchenko S., 2006, Nuclear Physics B-Proceedings Supplements, 151.1, 143.

fig1

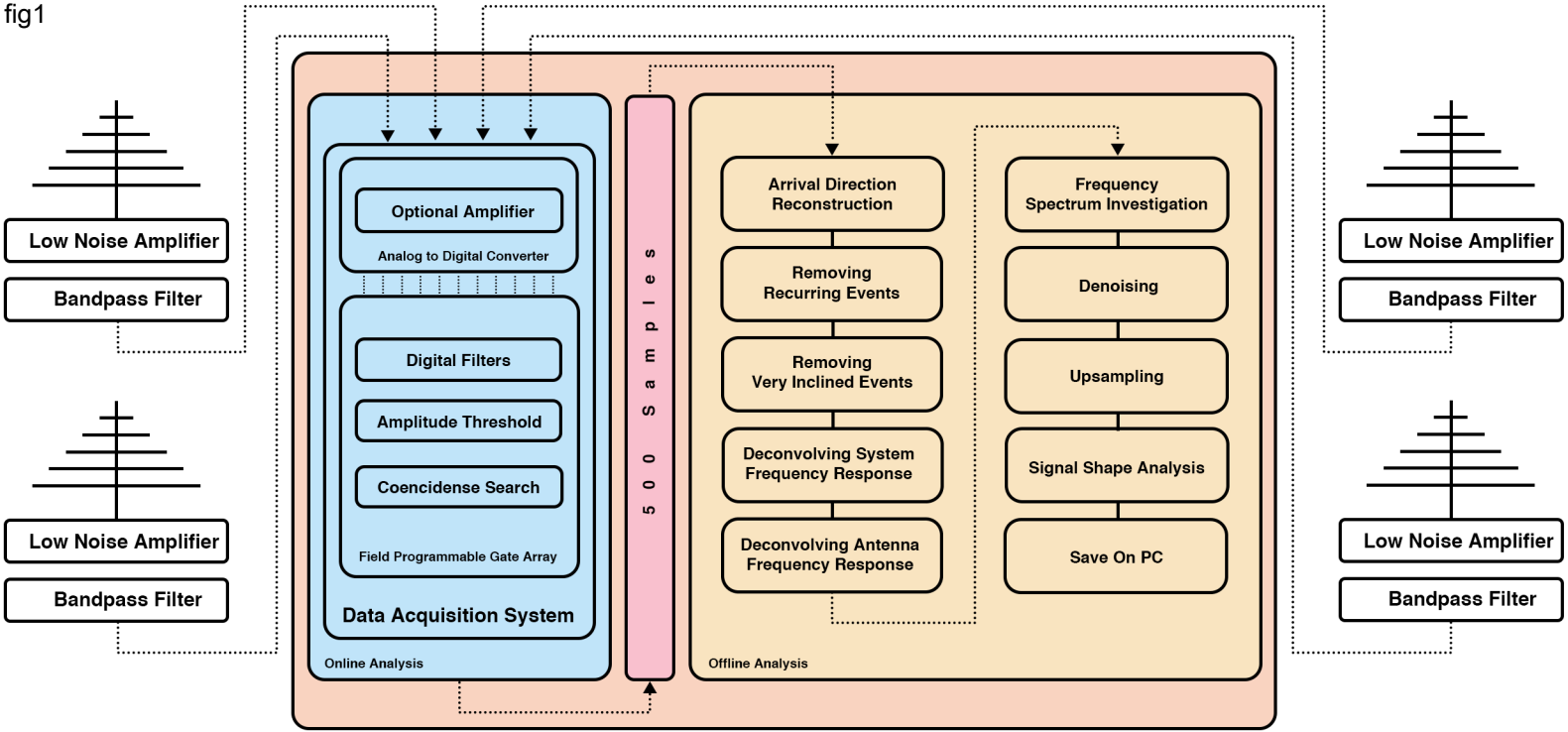
Low Noise Amplifier
Bandpass Filter
Low Noise Amplifier
Bandpass Filter
Low Noise Amplifier
Bandpass Filter
Low Noise Amplifier
Bandpass Filter
Optional Amplifier
Analog to Digital Converter
Digital Filters
Amplitude Threshold
Coencidense Search
Field Programmable Gate Array
Data Acquisition System
Online Analysis
500 Samples
Arrival Direction Reconstruction
Removing Recurring Events
Removing Very Inclined Events
Deconvolving System Frequency Response
Deconvolving Antenna Frequency Response
Frequency Spectrum Investigation
Denoising
Upsampling
Signal Shape Analysis
Save On PC
Offline Analysis

fig10

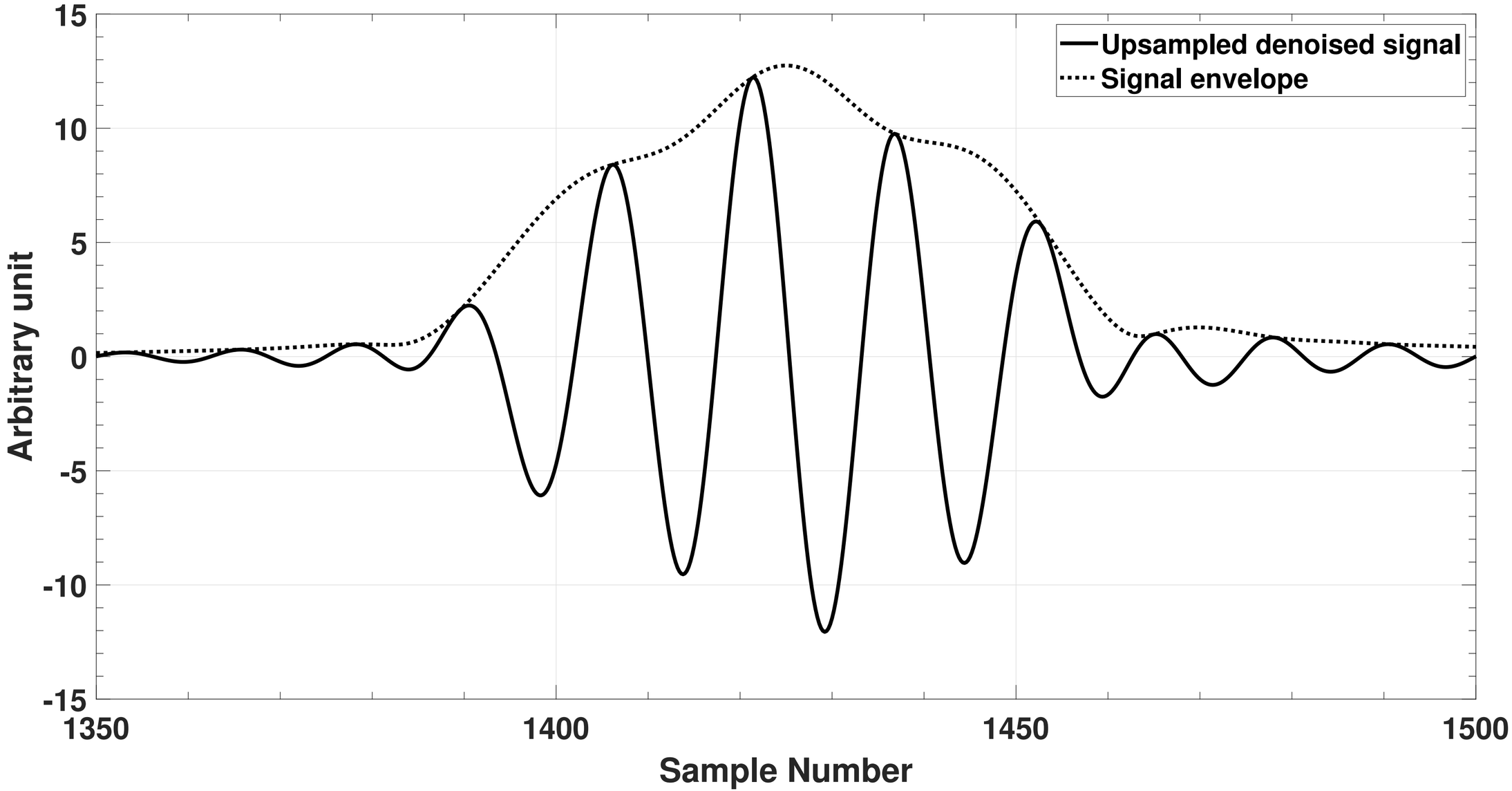
Upsampled denoised signal
Signal envelope
15
10
5
0
-5
-10
-15
Arbitrary unit
1350
1400
1450
1500
Sample Number

fig2

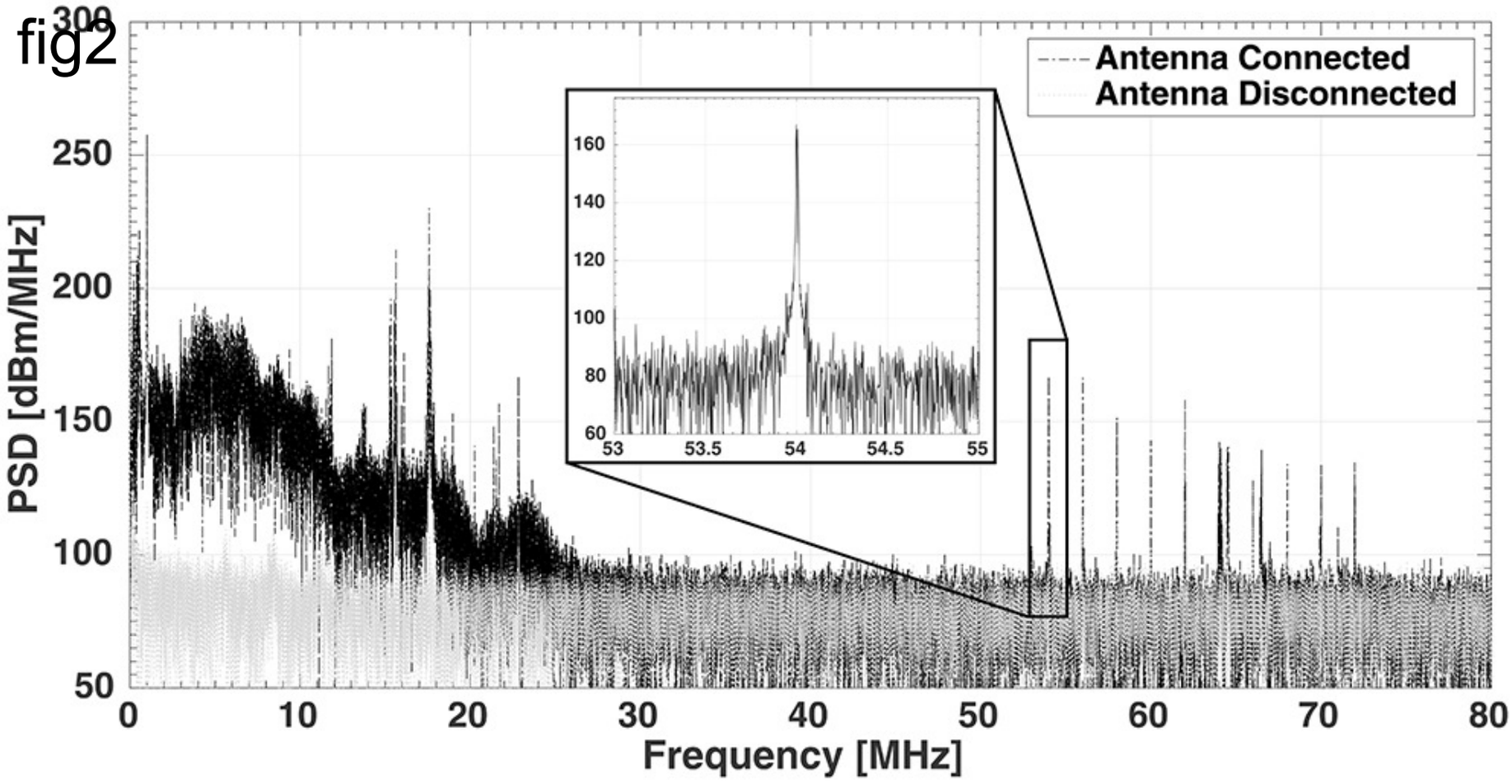
Antenna Connected
Antenna Disconnected
PSD [dBm/MHz]
Frequency [MHz]
300
250
200
150
100
50
0
10
20
30
40
50
60
70
80
160
140
120
100
80
60
53
53.5
54
54.5
55

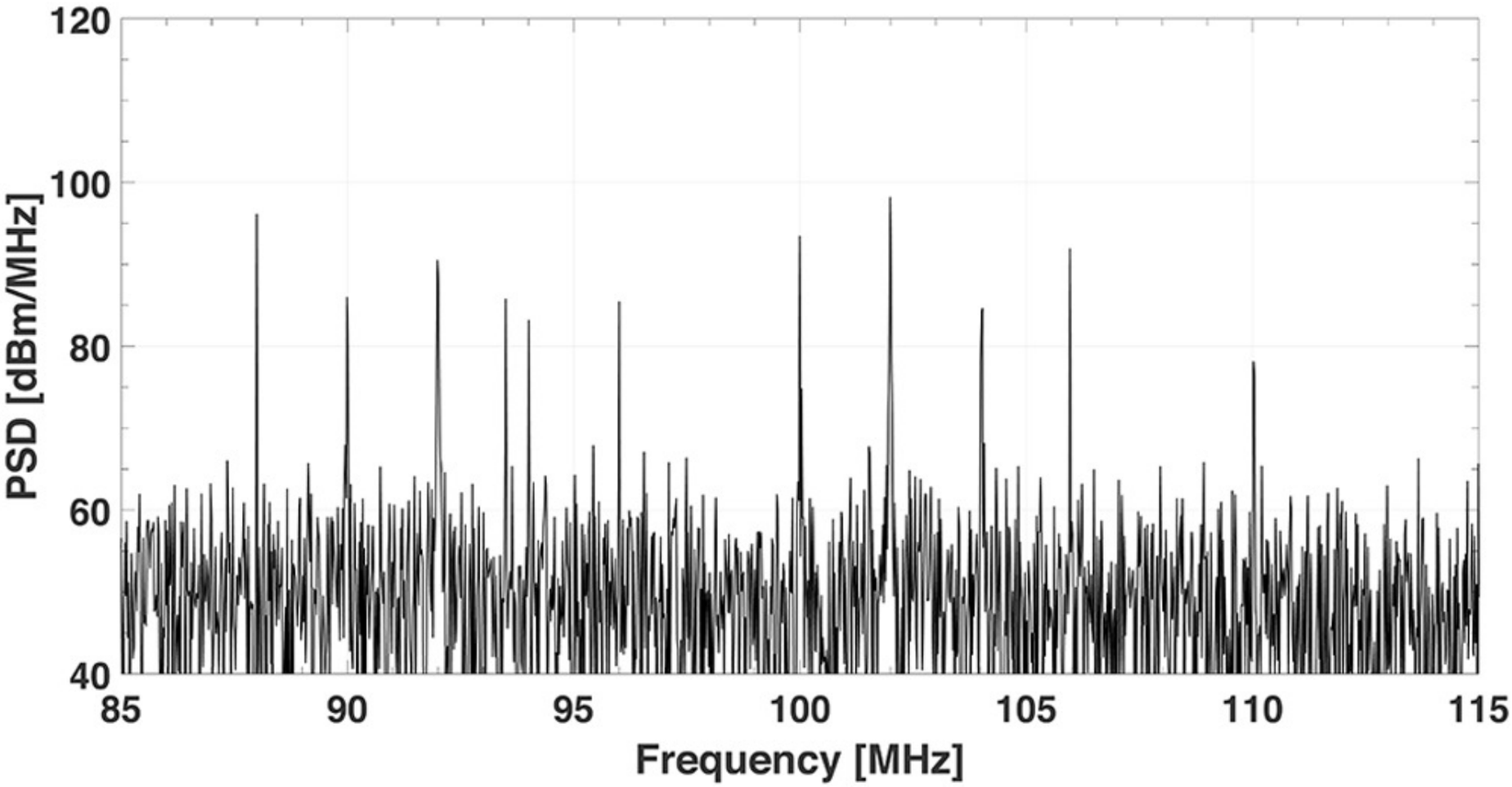
PSD [dBm/MHz]
Frequency [MHz]
120
100
80
60
40
85
90
95
100
105
110
115

fig3

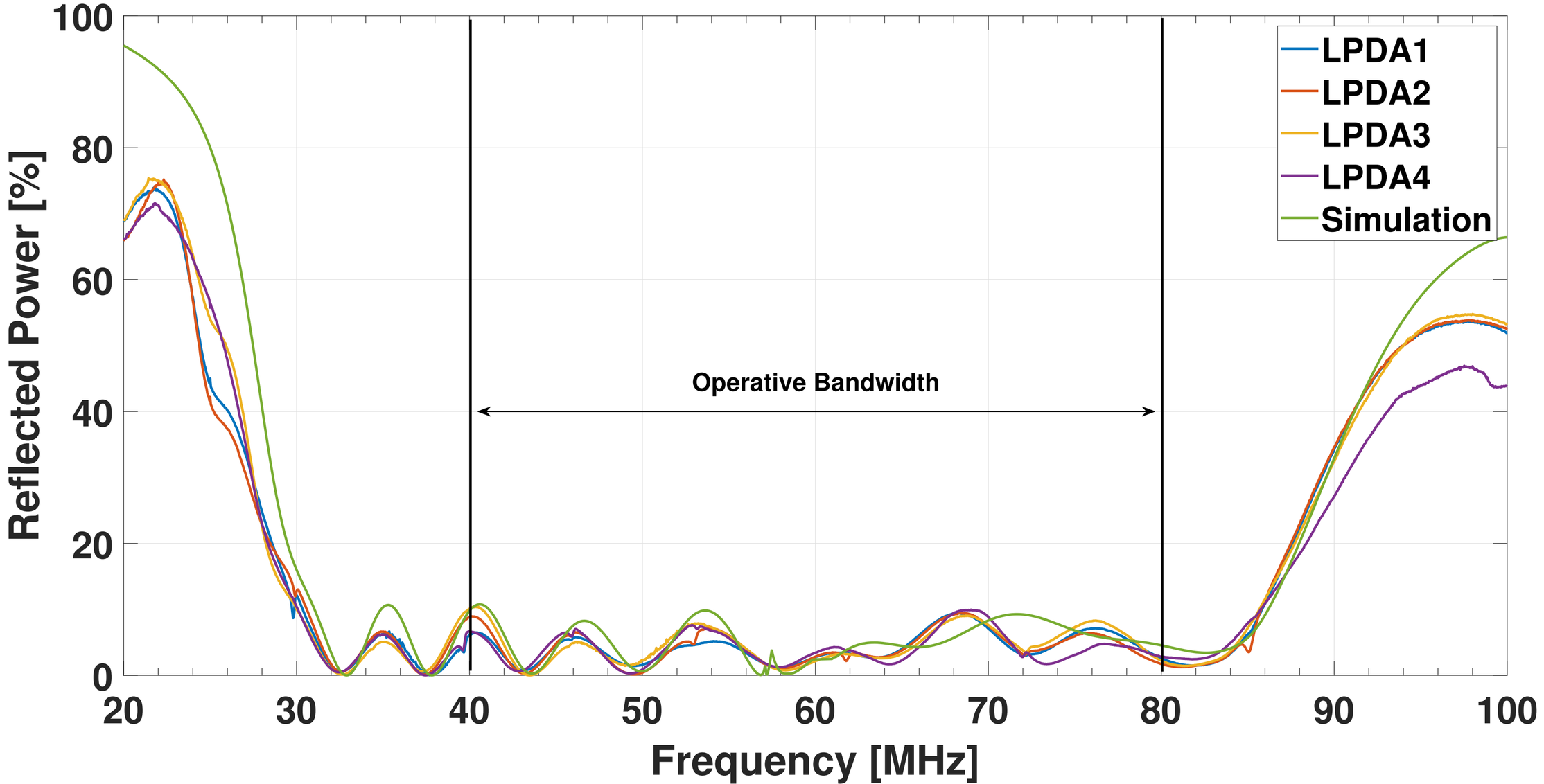
100
80
60
40
20
0
Reflected Power [%]
20
30
40
50
60
70
80
90
100
Frequency [MHz]
Operative Bandwidth
LPDA1
LPDA2
LPDA3
LPDA4
Simulation

fig4

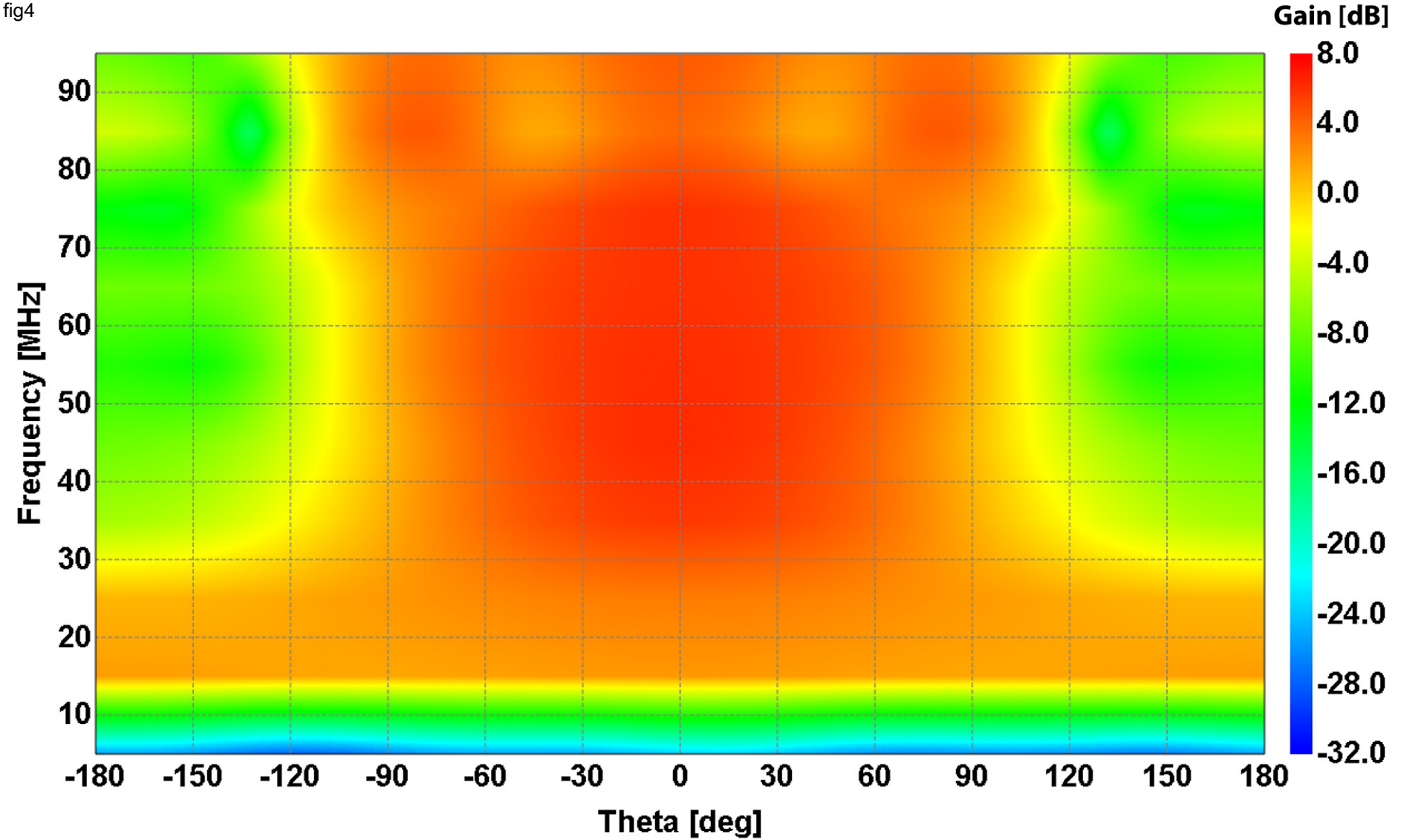
Gain [dB]
8.0
4.0
0.0
-4.0
-8.0
-12.0
-16.0
-20.0
-24.0
-28.0
-32.0
Frequency [MHz]
90
80
70
60
50
40
30
20
10
-180
-150
-120
-90
-60
-30
0
30
60
90
120
150
180
Theta [deg]

fig5

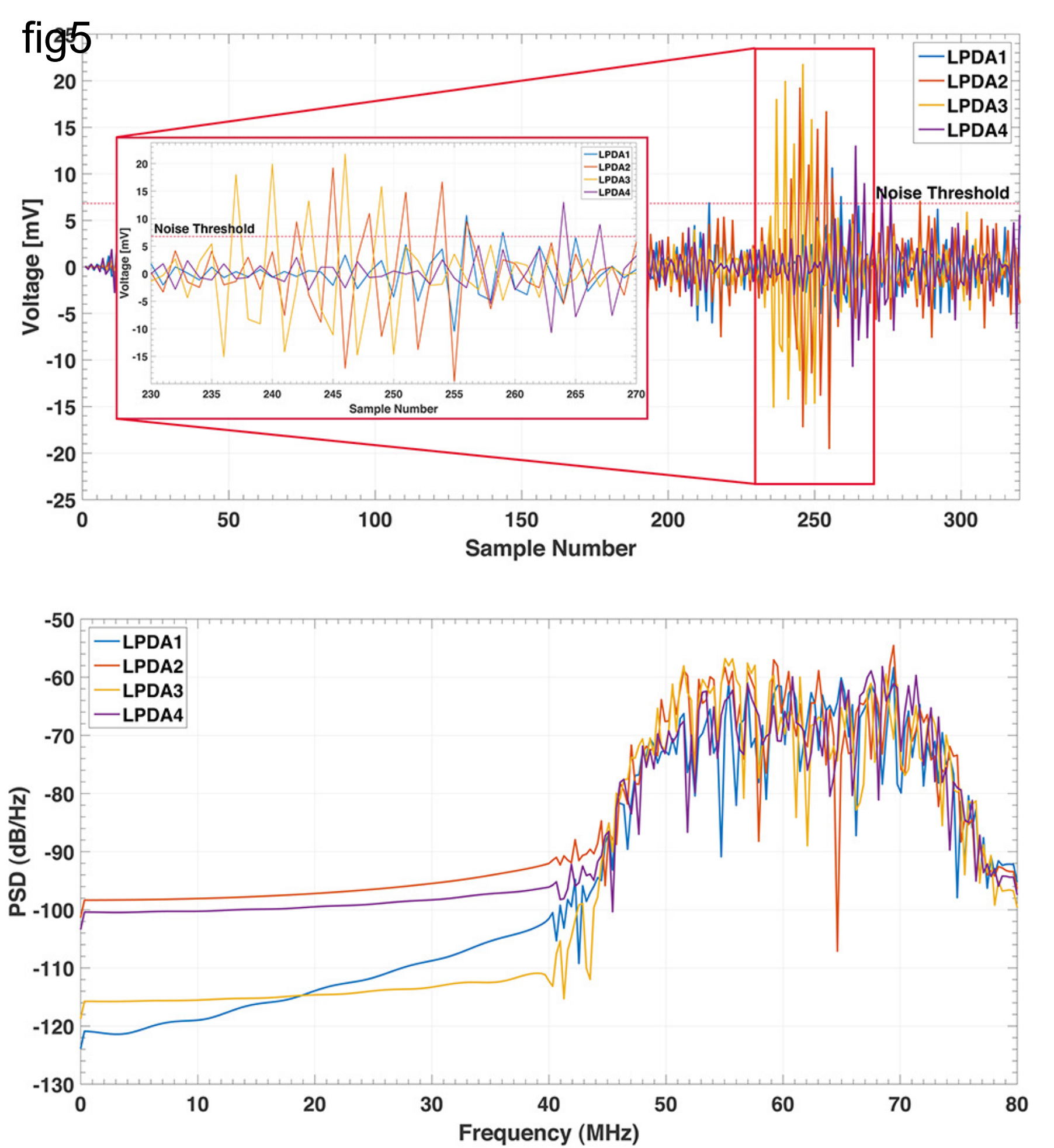
LPDA1
LPDA2
LPDA3
LPDA4
Noise Threshold
Voltage [mV]
Sample Number
PSD (dB/Hz)
Frequency (MHz)

fig6

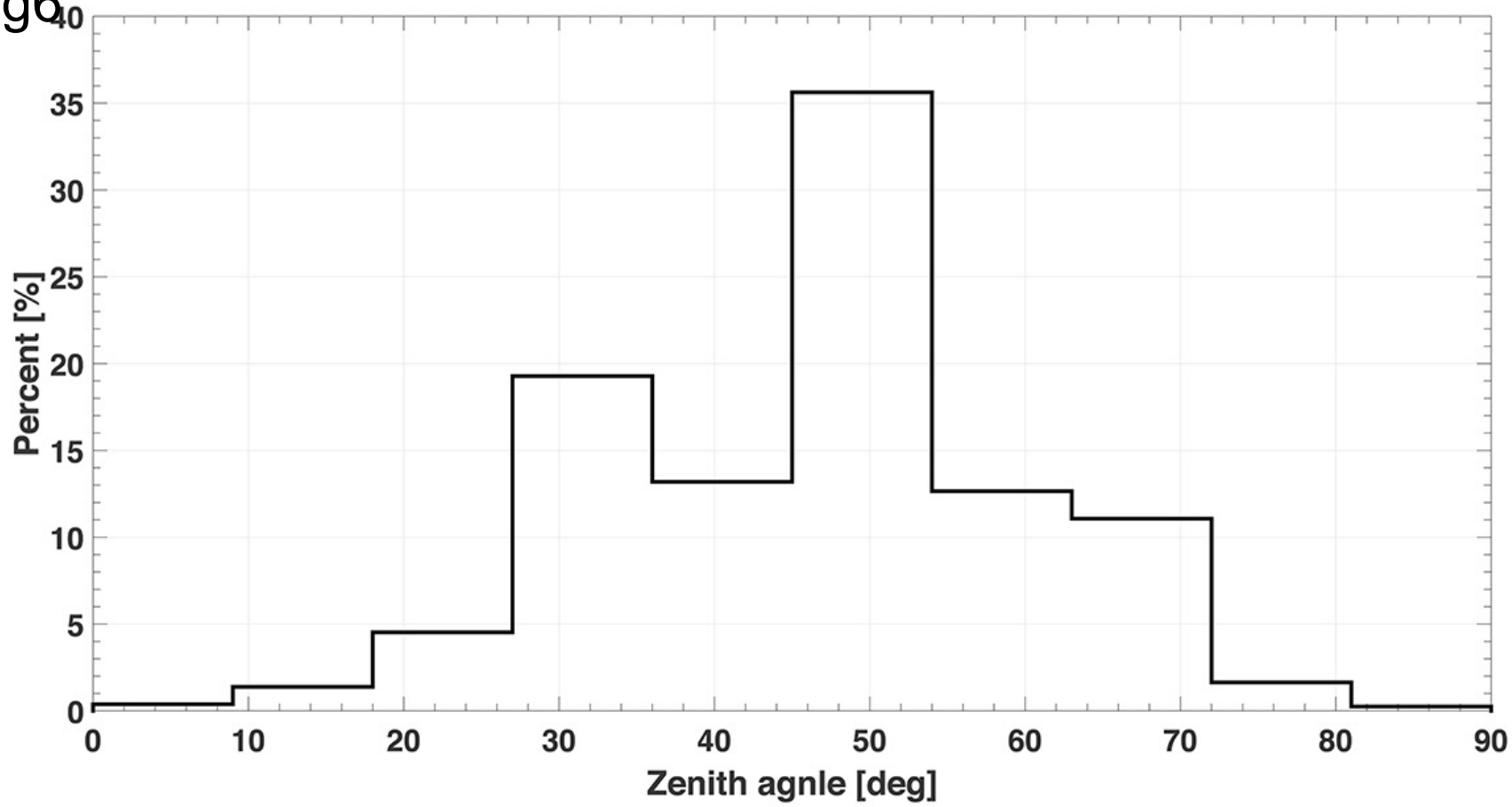
Percent [%]
0
5
10
15
20
25
30
35
40
0
10
20
30
40
50
60
70
80
90
Zenith agnle [deg]

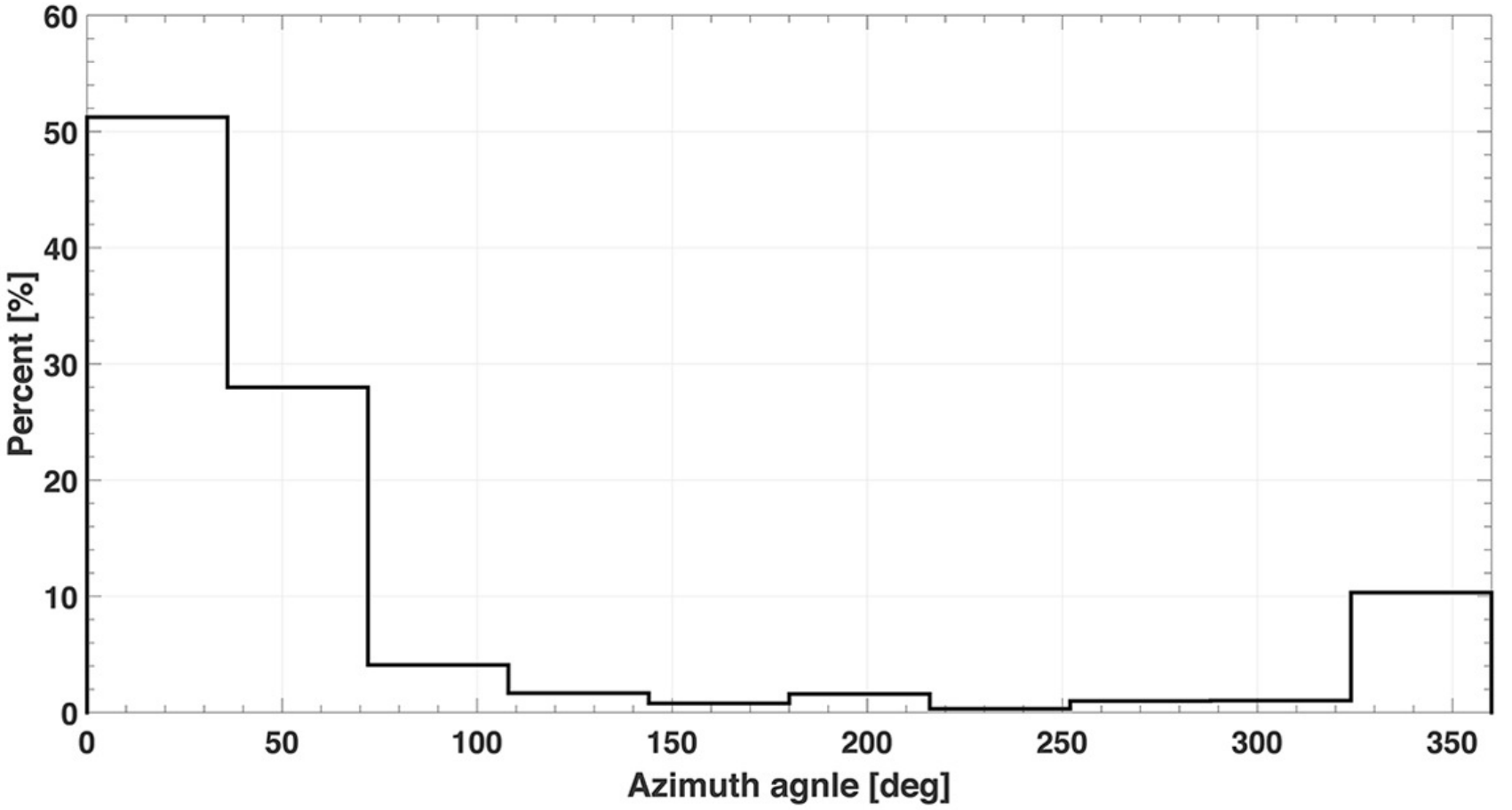
Percent [%]
0
10
20
30
40
50
60
0
50
100
150
200
250
300
350
Azimuth agnle [deg]

fig7

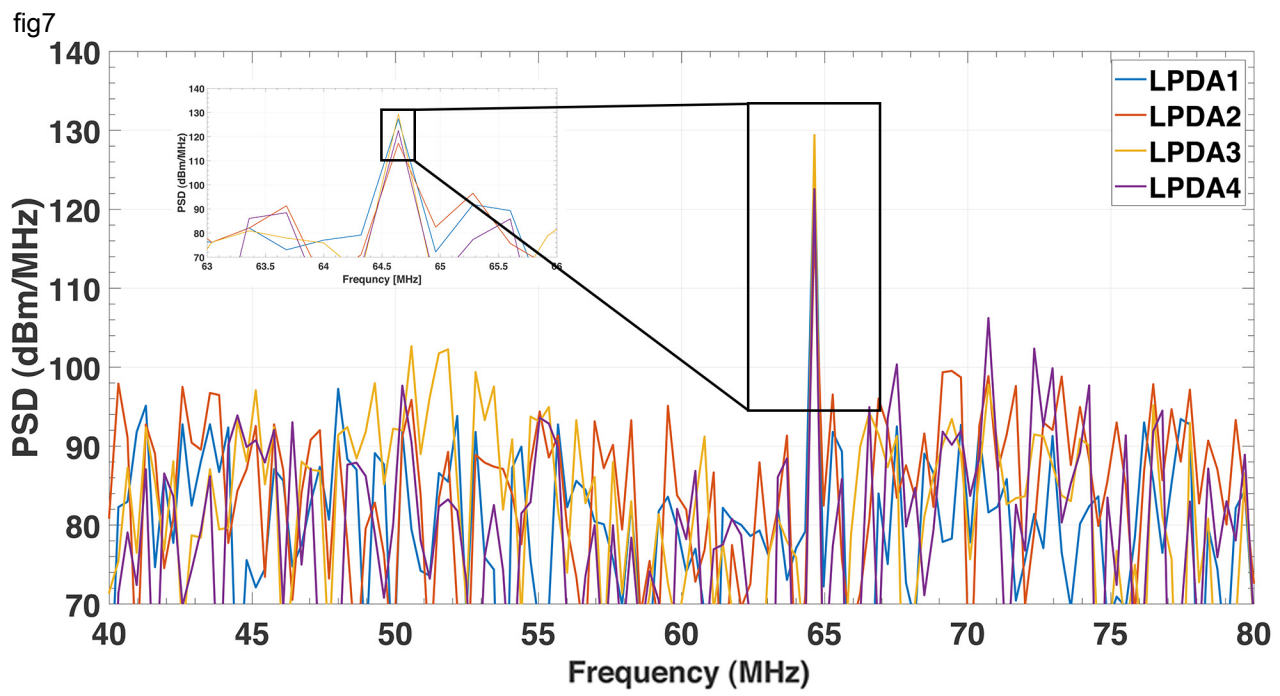
LPDA1
LPDA2
LPDA3
LPDA4
PSD (dBm/MHz)
Frequency (MHz)
140
130
120
110
100
90
80
70
40
45
50
55
60
65
70
75
80
PSD (dBm/MHz)
Frequncy [MHz]
63
63.5
64
64.5
65
65.5
66

fig8

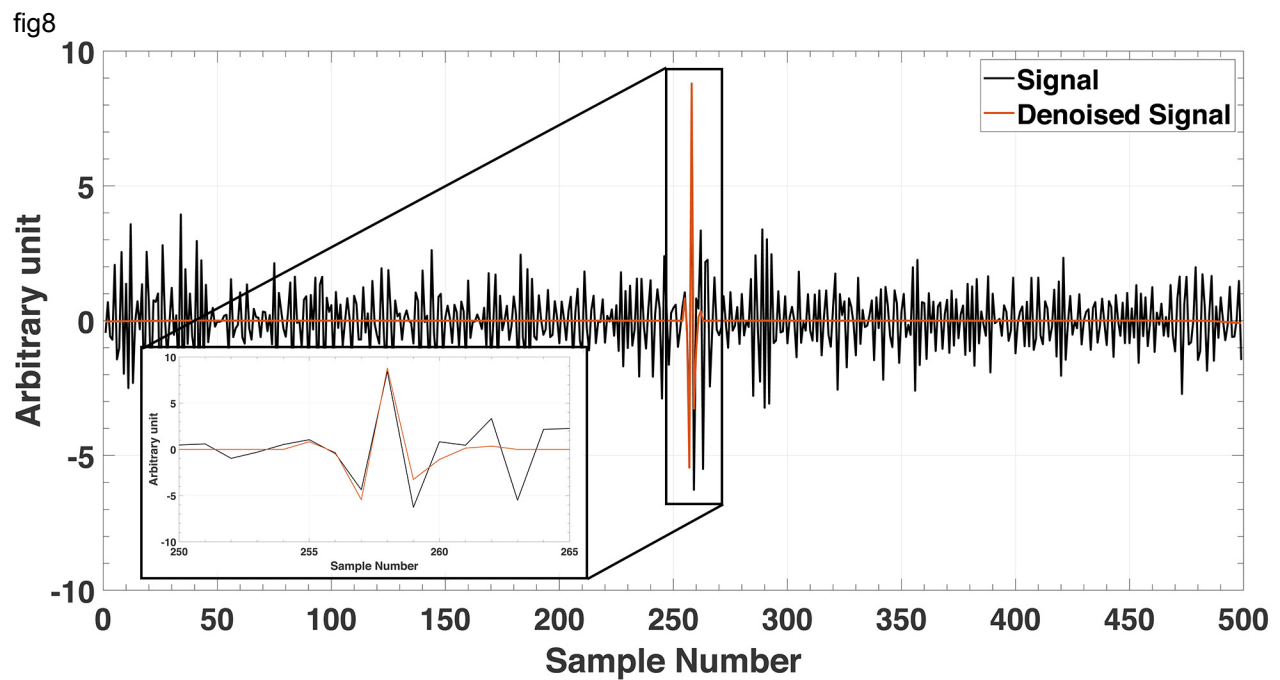
Signal
Denoised Signal
Arbitrary unit
Sample Number
10
5
0
-5
-10
0
50
100
150
200
250
300
350
400
450
500
Arbitrary unit
Sample Number
10
5
0
-5
-10
250
255
260
265

fig9

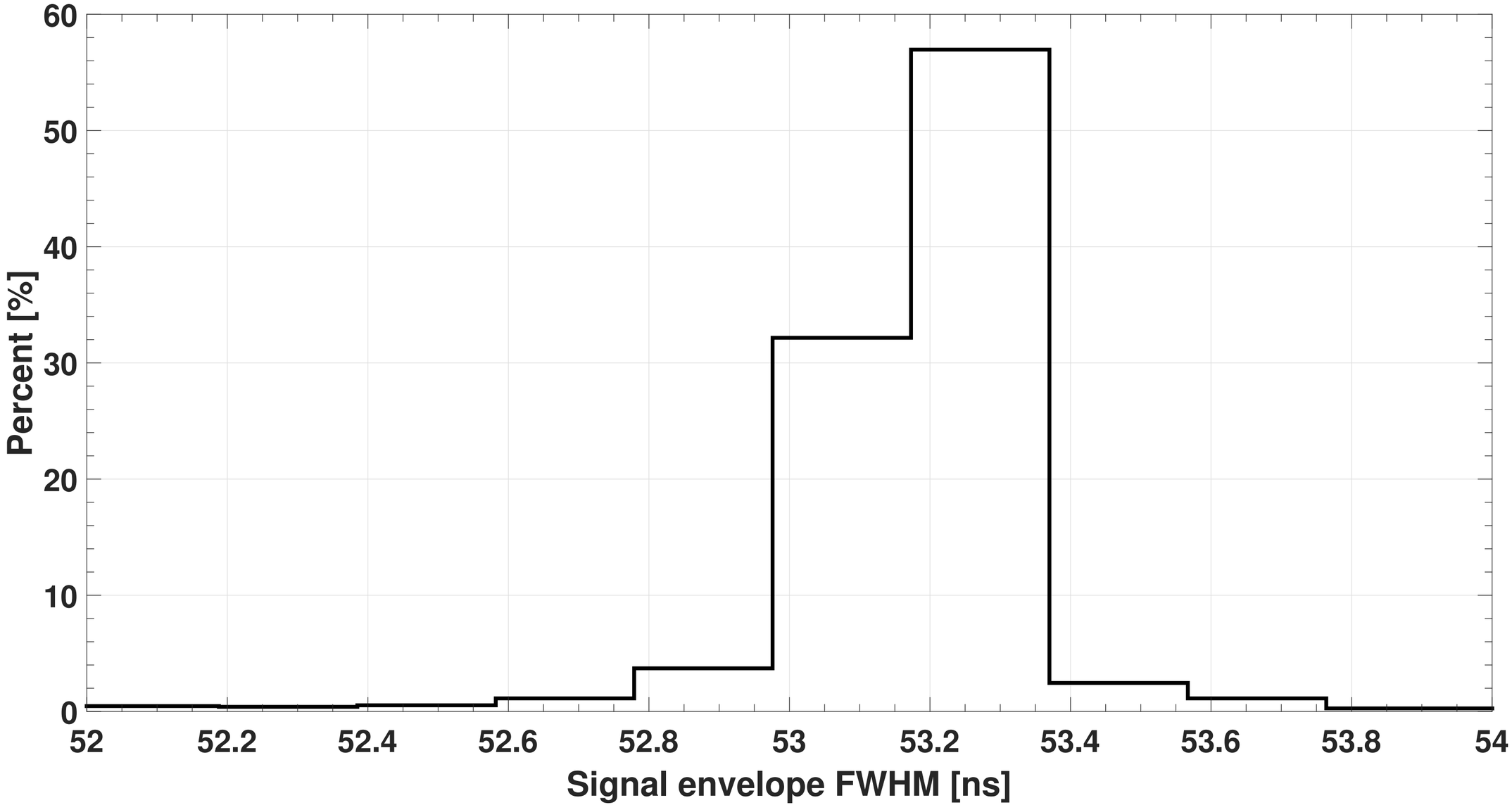
60
50
40
30
20
10
0
Percent [%]
52
52.2
52.4
52.6
52.8
53
53.2
53.4
53.6
53.8
54
Signal envelope FWHM [ns]